



## Theoretical investigation of the molecular structure and molecular docking of naratriptan

WENDOLYNE LÓPEZ-OROZO<sup>1</sup>, CLARA HILDA RIOS REYES<sup>2</sup>  
and LUIS HUMBERTO MENDOZA HUIZAR<sup>1\*</sup>

<sup>1</sup>Universidad Autónoma del Estado de Hidalgo, Academic Area of Chemistry, Carretera Pachuca-Tulancingo Km. 4.5 Mineral de la Reforma, Hgo, México and <sup>2</sup>Universidad Lasalle Pachuca, Calle Belisario Domínguez 202, Centro, 42000 Pachuca de Soto, Hgo. México

(Received 29 December 2019, revised 10 April, accepted 11 May 2020)

**Abstract:** In this work, a computational chemical study of the naratriptan was carried out at the X/DGDZVP (where X = B3LYP, M06, M06L and ωB97XD) level of theory, the results suggest the existence of two possible conformers in the aqueous phase. The evaluation of the global and local reactivity descriptors indicates that both conformers show the same chemical behaviour. The docking studies reveal that both conformers bind to TYR359 residue of the 5HT<sub>1B</sub> receptor. Also, the first conformer binds to the receptor through THR209 and THR213 while the second one through THR209 and SER 212.

**Keywords:** triptanes; reactivity; Fukui; docking; migraine.

### INTRODUCTION

Migraine is a common neurovascular disorder,<sup>1,2</sup> characterized by moderate to severe headaches, which in some cases are accompanied by dizziness, nausea,<sup>2,3</sup> hypersensitivity to light, sounds, and odours<sup>2</sup>. According to studies reported in the literature, migraine is considered a hereditary dysfunction of sensory modulation networks.<sup>1,4</sup> In this sense, the mitigation of the discomfort caused by migraine can be done through drugs capable of reducing the activity of secondary neurons, which allows effective treatment of pain caused by this condition.<sup>4</sup> In this sense, Naratriptan (*N*-methyl-3-(1-methyl-4-piperidinyl)-1*H*-indol-5-ethane) is a second generation triptan drug,<sup>5,6</sup> see Fig. 1, selective for the 5-hydroxytryptamine (5HT) receptor subtype and is able of causing a therapeutic effect in migraine patients.<sup>7</sup> Also, naratriptan has no clinical effects on blood pressure or heart rate,<sup>8</sup> and has a long duration of action with very good tolerability and a high oral bioavailability. Moreover, naratriptan is excreted largely as unchanged drug in the urine,<sup>9</sup> which eliminates the possibility to generate metabolites with

\*Corresponding author. E-mail: hhuizar@uaeh.edu.mx  
<https://doi.org/10.2298/JSC191229025L>

undesirable side effects. Here, it is interesting to mention that some triptanes exhibit polymorphism, which generate structures with different physicochemical behaviour in properties of pharmaceutical interest.<sup>10</sup> However, for naratriptan only one principal conformer has been reported (National Center for Biotechnology Information. PubChem Database; naratriptan, CID = 4440, 2019), although, other investigations suggest the existence of polymorphic forms of naratriptan, in solid phase, but without report of the structures.<sup>11</sup> To our knowledge, a computational chemical study of naratriptan to evaluate its global and local reactivity descriptors in aqueous phase is still missing. We consider that this kind of study will contribute to get a better understanding of the chemical behaviour of this important serotonergic agonist and a vasoconstrictor agent, in the aqueous phase.

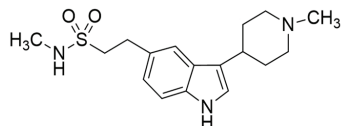


Figure 1. Naratriptan (*N*-methyl-3-(1-methyl-4-piperidinyl)-1*H*-indol-5-ethane) structure.

### Theory

*Global reactivity parameters.* Global reactivity parameters such as the electronic chemical potential ( $\mu$ ), electrophilicity ( $\chi$ ), hardness ( $\eta$ ) and the electrophilicity index ( $\omega$ ) are used to understand the general chemical behaviour of a molecule.<sup>12,13</sup> They can be evaluated within the framework of the DFT through Eqs. (1)–(4), respectively:<sup>14–17</sup>

$$\mu = \left( \frac{\partial E}{\partial N} \right)_{V(r)} = -\frac{1}{2}(I + A) = \frac{1}{2}(\epsilon_L + \epsilon_H) \quad (1)$$

$$\chi = -\mu \quad (2)$$

$$\eta = \left( \frac{\partial \mu}{\partial N} \right)_{V(r)} = \left( \frac{\partial^2 E}{\partial N^2} \right)_{V(r)} = (I - A) = (\epsilon_L - \epsilon_H) \quad (3)$$

$$\omega = \frac{\mu^2}{2\eta} \quad (4)$$

In these equations, the variables  $E$ ,  $N$  and  $V(r)$  are the energy, number of electrons and the external potential exerted by the nuclei, respectively.  $I$  is the ionization potential while  $A$  corresponds to the electronic affinity. Also, some reports suggest that the Koopmans' theorem may become valid for calculations of the global reactivity parameters at the DFT level.<sup>15,18,19</sup> Under this approximation,  $A$  is related to the minus lowest unoccupied molecular orbital (LUMO) energy ( $-\epsilon_L$ ), while  $I$  is associated with the minus highest occupied molecular orbital (HOMO) energy ( $-\epsilon_H$ ).<sup>15,18,19</sup> On the other hand, the electronic chemical potential is associated to the escaping tendency of an electron,<sup>18</sup>  $\eta$  is related to the stability of the molecular system;<sup>14,15</sup> while  $\omega$  measures the susceptibility of chemical species to accept electrons.<sup>19</sup> Thus, low values of  $\omega$  suggest a good nucleophile while higher values indicate the presence of a good electrophile. Besides, it is possible to define the electrodonating ( $\omega$ ) and electroaccepting ( $\omega^+$ ) powers as:<sup>19</sup>

$$\omega^- = \frac{(\mu^-)^2}{2\eta} = \frac{(-(3I+A)/4)^2}{2(I-A)} = \frac{(-(3\varepsilon_L + \varepsilon_H)/4)^2}{2(\varepsilon_L - \varepsilon_H)} \quad (5)$$

$$\omega^+ = \frac{(\mu^+)^2}{2\eta} = \frac{(-(I+3A)/4)^2}{2(I-A)} = \frac{(-(\varepsilon_L + 3\varepsilon_H)/4)^2}{2(\varepsilon_L - \varepsilon_H)} \quad (6)$$

*Local reactivity parameters.* Probably, the Fukui function( $f(r)$ ) is one of the local parameters most used to identify the more reactive regions or sites on a molecular system,<sup>20,21</sup> which is defined as:<sup>22</sup>

$$f(r) = \left( \frac{\partial \rho(r)}{\partial N} \right)_{v(r)} = \left( \frac{\partial \mu(r)}{\partial v(r)} \right) \quad (7)$$

where  $\rho(r)$  is the electronic density. From Eq. (7), it is clear that FF indicates the regions where a chemical species will change its electronic density, when the number of electrons is modified, which is useful to identify the preferred either molecular regions, susceptible to electrophilic or nucleophilic attacks.<sup>21</sup> In this sense, FF can be evaluated using different approximations, but the more employed are: a) frozen core approximation (FC),<sup>22</sup> b) finite differences (FD)<sup>22</sup> and c) atomic charges.<sup>23</sup> In the FC approximation, FF for electrophilic and nucleophilic attacks can be evaluated through the Eqs. (8) and (9), respectively:

$$f^-(r) = \varphi_H^*(r)\varphi_H(r) = \rho_H(r) \quad (8)$$

$$f^+(r) = \varphi_L^*(r)\varphi_L(r) = \rho_L(r) \quad (9)$$

In these equations,  $\rho_H(r)$  is the electronic density of the HOMO, while  $\rho_L(r)$  is the electronic density of the LUMO.

In the FD approximation, FF the electrophilic, nucleophilic and free radical attacks can be evaluated by Eqs. (10)–(12), respectively:

$$f^-(r) = \rho_N(r) - \rho_{(N-1)}(r) \quad (10)$$

$$f^+(r) = \rho_{N+1}(r) - \rho_N(r) \quad (11)$$

$$f^0(r) = \frac{1}{2} [\rho_{N+1}(r) - \rho_{N-1}(r)] \quad (12)$$

where  $\rho_{N+1}(r)$ ,  $\rho_N(r)$ , and  $\rho_{N-1}(r)$  correspond to the electronic density of the anion, neutral and cationic chemical species, respectively.

Also, it is possible to condense the FF to an atomic position, employing the values of the atomic charges, as is shown in Eqs. (13)–(15):

$$f_j^-(r) = q_{j(N-1)} - q_{j(N)} \quad (13)$$

$$f_j^+(r) = q_{j(N)} - q_{j(N+1)} \quad (14)$$

$$f_j^0(r) = \frac{1}{2} (q_{j(N-1)} - q_{j(N+1)}) \quad (15)$$

where  $q_j$  is the atomic charge (evaluated from Löwdin, Mulliken or Hirshfeld population analysis, electrostatic derived charge, etc.) at the  $j_{th}$  atomic site in the neutral ( $N$ ), anionic ( $N+1$ ) or cationic ( $N-1$ ) chemical species. In the present work, Hirshfeld population have been used to evaluate the values of the Condensed Fukui function(CFF), because Hirshfeld charges

are less sensitive to the basis set size employed, in comparison to the Löwdin or Mulliken charges. Additionally, the CFF values obtained through Hirshfeld charges are consistent when different electronic structure methods are employed.<sup>24</sup>

#### COMPUTATIONAL METHODOLOGY

The conformational analysis of naratriptan was carried out using molecular mechanics, and molecular dynamics (not shown). The optimal conformations of naratriptan were subjected to full geometry optimization in the aqueous phase employing the X/DGDZVP,<sup>25</sup> (where X = B3LYP,<sup>26,27</sup> M06,<sup>28</sup> M06L<sup>29</sup> and ωB97XD<sup>30</sup>) level of theory. Solvent phase optimization were carried out using the polarizable continuum model (PCM) developed by Tomasi and coworkers.<sup>31,32</sup> In all cases the vibrational frequencies were calculated to make sure that the stationary points were minima in the potential energy surface. All the quantum calculations reported here were performed with the package Gaussian 09,<sup>33</sup> and visualized with the GaussView V.3.09,<sup>34</sup> Arguslab,<sup>35</sup> Gabedit<sup>36</sup> and Multwfn<sup>37</sup> packages. Docking study was done through the PYRX,<sup>38</sup> and Autodock Vina<sup>39</sup> packages and visualized employing Chimera,<sup>40</sup> Pymol<sup>41</sup> and LigPlot+.<sup>42</sup>

#### RESULTS AND DISCUSSION

##### *Geometry optimization*

From the conformational analysis, it was possible to identify the two lowest energy conformations of naratriptan, see Fig. 2. These conformations were optimized without restrictions at the X/DGDZVP<sup>25</sup> (where X = B3LYP,<sup>26,27</sup> M06,<sup>28</sup> M06L<sup>29</sup> and ωB97XD<sup>30</sup>) level of theory, in the gas and aqueous phases. Here, it is important to mention that significant differences were not obtained, neither in distances nor angles, when the solvent effect was considered at the different levels of theory employed in this work. All frequency values calculated at the X/DGDZVP<sup>25</sup> (where X = B3LYP,<sup>26,27</sup> M06,<sup>28</sup> M06L<sup>29</sup> and ωB97XD<sup>30</sup>) level of theory were positive in the aqueous phase and are in good agreement with the values reported in the literature;<sup>43</sup> which suggests that the level of theory employed is able to predict the electronic properties of naratriptan. A summary of the main bands is depicted in Fig. S-1 of the Supplementary material to this paper.

The total energy calculated in the gas phase, at the B3LYP/DGDZVP level of theory for the conformer I (Nar-I) is -1375.77174094 hartrees, while its HOMO–LUMO gap is 4.97 eV. The energy for conformer II (Nar-II) is -1375.77163113 hartrees and its HOMO–LUMO gap is 4.95 eV. An energy difference of 0.067 kcal\* mol<sup>-1</sup> suggests that both structures are equivalent. In aqueous phase, the energies of Nar-I and Nar-II are -1375.79387626 and -1375.79377903 hartrees respectively, with a difference of 0.061 kcal mol<sup>-1</sup>. Also, the energy difference between the naratriptan in the gas phase in comparison to the same molecule in aqueous phase is 13.9 kcal mol<sup>-1</sup>, in both cases, which suggests that Nar-I and Nar-II have the same solvation energy.

---

\* 1 kcal = 4184 J

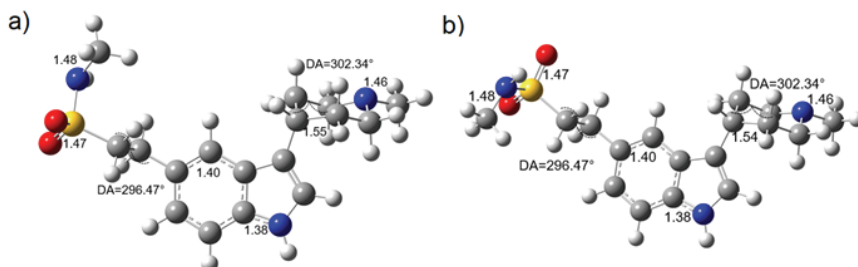


Fig. 2. Naratriptan conformers: a) Nar-I and b) Nar-II, optimized at the B3LYP/DGDZVP level of theory in the aqueous phase employing the PCM solvation model. Bond distances are given in Å; DA = dihedral angle.

From Fig. 2, it is possible to observe a different orientation of the sulfonamide group in Nar-I in comparison to Nar-II, which may be caused by the presence of noncovalent interactions. In this sense, it is possible to determine these interactions through the *NCI* index proposed by Johnson *et al.*,<sup>44</sup> through the plot of the reduced density gradient ( $s(r)$ ), versus  $\rho(r)$ , where  $s(r)$  is given by:

$$s(r) = \frac{1}{2(3\pi^2)^{1/3}} \frac{|\nabla\rho(r)|}{\rho(r)^{4/3}} \quad (16)$$

According to the *NCI* index in regions far from the molecule the density decays to zero exponentially and in consequence the reduced gradient will have large positive values, while that in regions of covalent bonding and noncovalent interactions, the reduced gradient will have values close to zero.<sup>44</sup> Fig. S-2 of the Supplementary material shows a 2D *NCI* plot for Nar-I and Nar-II and at the low reduced gradient region both plots are exhibiting a similar number of spikes, but at 0.009 for Nar-I, there is an additional interaction which is not present in Nar-II. This interaction may be related to a noncovalent interaction. In order to elucidate the nature of this interaction the  $s(r)$  isosurfaces of Nar-I and Nar-II were plotted, see Fig. S-3 of the Supplementary material, where it is shown that the additional interaction observed in the 2D *NCI* plot is corresponding to a hydrogen bond.

#### *Global reactivity parameters*

The global reactivity descriptors for Nar-I and Nar-II were evaluated employing the Eqs. (1)–(6) and they are reported in Table I. Note that the values of all the descriptors for Nar-I and Nar-II are similar when they are compared at the same level of theory, which suggests the same global chemical behaviour of the two conformers.

TABLE I. Global reactivity parameters, for Nar-I and Nar-II, evaluated at the X/DGDZVP<sup>25</sup> (where X = B3LYP,<sup>26,27</sup> M06,<sup>28</sup> M06L<sup>29</sup> and ωB97XD<sup>30</sup>) level of theory and in the aqueous phase, employing Eqs. (1)–(6). The values between parentheses corresponds to the values calculated employing the Koopmans' theorem.

Procedure	<i>I</i> / eV	<i>A</i> / eV	$\mu$ / eV	$\eta$ / eV	$\chi$ / eV	$\omega$ / eV	$\omega^+$ / eV	$\omega^-$ / eV	$\Delta\omega$ / eV
Nar-I									
B3LYP	5.59 (5.69)	0.89 (0.75)	-3.24 (-3.22)	4.69 (4.94)	3.24 (3.22)	1.12 (1.05)	0.46 (0.40)	2.08 (2.01)	2.53 (2.40)
M06	5.68 (5.98)	0.95 (0.59)	-3.32 (-3.29)	4.73 (5.39)	3.32 (3.29)	1.16 (1.00)	0.48 (0.35)	2.14 (1.99)	2.62 (2.34)
M06L	5.37 (5.01)	0.86 (1.20)	-3.11 (3.10)	4.51 (3.81)	3.11 (3.10)	1.07 (1.26)	0.44 (0.61)	1.99 (2.16)	2.43 (2.76)
ωB97XD	5.79 (7.62)	0.82 (-1.08)	-3.31 (-3.27)	4.97 (8.70)	3.31 (3.27)	1.10 (0.62)	0.43 (0.07)	2.08 (1.70)	2.51 (1.77)
Nar-II									
B3LYP	5.58 (5.68)	0.89 (0.74)	-3.23 (-3.21)	4.69 (4.94)	3.23 (3.21)	1.12 (1.04)	0.45 (0.40)	2.07 (2.00)	2.52 (2.40)
M06	5.67 (5.97)	0.93 (0.57)	-3.30 (-3.27)	4.74 (5.40)	3.30 (3.27)	1.15 (0.99)	0.47 (0.34)	2.13 (1.98)	2.60 (2.32)
M06L	5.36 (5.00)	0.84 (1.18)	-3.10 (-3.09)	4.52 (3.83)	3.10 (3.09)	1.06 (1.25)	0.43 (0.59)	1.98 (2.14)	2.41 (2.73)
ωB97XD	5.78 (7.61)	0.81 (-1.09)	-3.30 (-3.26)	4.98 (8.71)	3.30 (3.26)	1.09 (0.61)	0.42 (0.07)	2.07 (1.70)	2.49 (1.76)

### Local reactivity parameters

The local reactivity of a molecular system can be evaluated through the Fukui Function, employing different approximations. Fig. S-4 of the Supplementary material shows the distribution of the electrophilic sites on Nar-I and Nar-II, employing the FC approximation. For both conformers the HOMO's distribution is located on the piperidinyl-indole section, while that LUMO's distribution is located on the indole ring. On the other hand, the Fukui function evaluated for Nar-I, employing the FD approximation (Eqs. (10)–(12)) is reported in Fig. 3. For the case of Nar-I, the more nucleophilic active sites are 2C, 3C and 11C, Fig. 3a, located on the piperidinyl-indole section; while the more electrophilic active sites are on the 10C, 12N and 16N atoms, see Fig. 3b. The more reactive sites to free radical attacks are located on 2C, 3C and 11C, see Fig. 3c. For the case of Nar-II, the more nucleophilic active sites are located on 2C, 3C and 11C (see Fig. S-5a of the Supplementary material). For electrophilic attacks, the more reactive sites are located are on 10C, 12N and 16N positions (Fig. S-5b), while for free radical attacks the more reactive sites are 2C, 3C and 11C (Fig. S-5c). From these results, it is clear that the more reactive sites are located on the same positions in both conformers, which is indicative that they are exhibiting the same reactivity at the local level to the different kind of attacks. Similar results to those obtained

in Figs. 3 and S-5 were obtained at the level of theory X/DGDZVP<sup>25</sup> (where X = B3LYP,<sup>26,27</sup> M06,<sup>28</sup> M06L<sup>29</sup> and ωB97XD<sup>30</sup>).

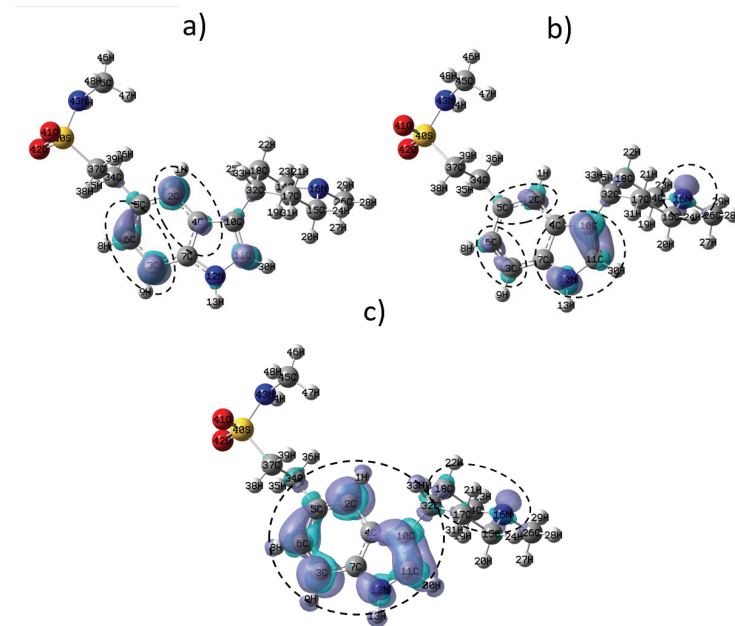


Fig. 3. Isosurfaces of the Fukui Functions for Nar-I according to Eqs. (10)–(12) at the B3LYP/DGDZVP level of theory employing the PCM solvation model. In the case of: a) nucleophilic, b) electrophilic and c) free radical attacks. In all cases the isosurfaces were obtained at 0.004 e/u.a.,<sup>3</sup> dashed circles show the more reactive zones in each molecule.

Also, it is possible to condense the Fukui function through Eqs. (13)–(15) to identify the point distribution of the active sites, because the higher values of CFF correspond to more reactive atoms in the referent molecule.<sup>45</sup> In the case of Eqs. (13)–(15), we used the Hirshfeld population to evaluate the values of CFF because the values obtained are non-negative.<sup>20,46</sup> The values of CFF for electrophilic, nucleophilic and free radical attacks at the B3LYP/DGDZVP level of theory employing the PCM solvation model for Nar-I are reported in Fig. 4. It is possible to observe that Nar-I exhibit more nucleophilic sites on 3C, 2C and 11C. In the electrophilic case, the more reactive sites are 10C, 11C and 12N while that for free radical attacks the more reactive sites are 2C, 3C and 11C. For the case of Nar-II, the more reactive sites, at the B3LYP/DGDZVP level of theory, are identical to those reported for Nar-I. Moreover, these results are coincident with those derived from the FF reported in Figs. 3 and S-5, which suggests that a change of the orientation of the sulfonamide group is not modifying the position of the more reactive sites on Nar-I and Nar-II.

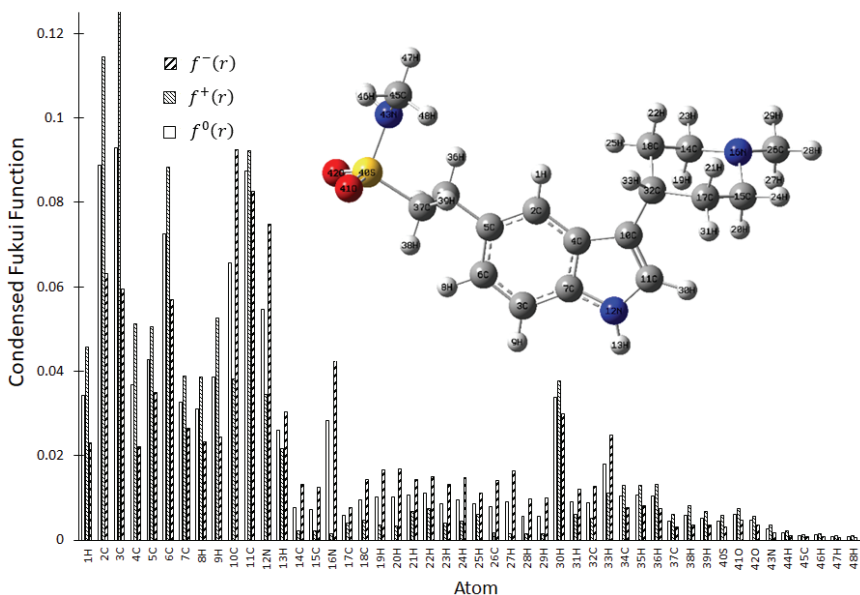


Fig. 4. Condensed Fukui function values for nucleophilic attacks on Nar-I at the X/DGDZVP (where X = B3LYP, M06, M06L and  $\omega$ B97XD) level of theory, in the aqueous phase employing Hirshfeld population and Eqs. (13)–(15).

In Figs. S-6–S-8 of the Supplementary material are reported the CFF of Nar-I for the nucleophilic, electrophilic and free radical attacks respectively, at the X/DGDZVP (where X = B3LYP, M06, M06L and WB97XD) level of theory, in the aqueous phase employing Hirshfeld population. For Nar-II the results are reported in Figs. S-9–S-11 of the Supplementary material, for the nucleophilic, the electrophilic and the free radical attacks, respectively. The local reactivity of Nar-I and Nar-II through the evaluation of the Fukui function employing the FC and FD approximations are in agreement with the CFF values.

Also, the chemical reactivity of Nar-I and Nar-II was analyzed through maps of the molecular electrostatic potential (MEP).<sup>47</sup> The MEPs for Nar-I and Nar-II are depicted in Fig. S-12 of the Supplementary material. In these images, the areas of negative potential (red colour), are characterized by an abundance of electrons while areas of positive potential (blue colour), are characterized by a relative lack of electrons. In the case of Nar-I and Nar-II the nitrogen atoms exhibit the lowest values of potential in comparison to the other atoms; consequently they have a higher electron density around it, and shows that the oxygen atoms as the places with the lowest potential and therefore they are the more electrophilic active sites. Additionally, in order to analyze the possible influence of the naratriptan conformers in their role as receptor agonists for treatment of migraine attacks, the optimal ligand/protein configuration and the binding affi-

nity for Nar-I and Nar-II with 5HT<sub>1B</sub> was analyzed. The receptor 5HT<sub>1B</sub> has been identified as the target of triptane receptor agonists.<sup>7</sup> Fig. S-13 of the Supplementary material shows the Nar-I/5HT<sub>1B</sub> configuration, where the binding energy is -9.3 kcal mol<sup>-1</sup> and Nar-II is interacting with 5HT<sub>1B</sub> with the same binding energy. In order to identify the residues in 5HT<sub>1B</sub>, which are interacting with naratriptan conformers, a 2D ligand interaction diagram was plotted employing the LigPlot+ software, see Fig. S-14 of the Supplementary material. Note that Nar-I establishes hydrogen bonds with Tyr359[O—H···N]; Thr213[O···N], Thr209[O···N] with a distance of 3.12, 3.07 and 3.18 Å, and hydrophobic interactions with the residues Asp352, Val201, Thr355, Phe330, Ile130, Ser212. On the other hand, Nar-II is forming hydrogen bonds with Tyr359[O—H···N], Ser212[O···N], Thr209[O···N] with a distance of 3.04, 2.97 and 3.24 Å, respectively, and hydrophobic interactions with the residues Asp 129, Leu126, Val200, Asp352 Ile130, Thr213 and Phe331. In both cases Nar-I and Nar-II are interacting with 5HT<sub>1B</sub> at the same active site, suggesting the same agonist effect.

#### CONCLUSION

In this work, we analyzed the chemical reactivity of two conformers of naratriptan in aqueous phase. According to the global descriptors both conformers exhibit the same global and local reactivity. The docking study indicates that Nar-I and Nar-II are binding with the 5HT<sub>1B</sub> receptor through TYR359 residue. Additionally, Nar-I binds to the receptor through THR209 and THR213 while Nar-II through THR209 and SER 212.

#### SUPPLEMENTARY MATERIAL

Additional data are available electronically at the pages of journal website: <https://www.shd-pub.org.rs/index.php/JSCS/index>, or from the corresponding author on request.

*Acknowledgements.* Authors gratefully acknowledge financial support from CONACYT (project CB2015-257823) and to the Universidad Autónoma del Estado de Hidalgo. Guanajuato National Laboratory (CONACyT 123732) is acknowledged for supercomputing resources. LHMH acknowledges to the SNI for the distinction of his membership and the stipend received.

ИЗВОД

ТЕОРИЈСКО ИСТРАЖИВАЊЕ МОЛЕКУЛСКЕ СТРУКТУРЕ И МОЛЕКУЛСКОГ ДОКИНГА НАРАТРИПТАНА

WENDOLYNE LÓPEZ-OROZO<sup>1</sup>, CLARA HILDA RIOS REYES<sup>2</sup> и LUIS HUMBERTO MENDOZA HUIZAR<sup>1</sup>

<sup>1</sup>Universidad Autónoma del Estado de Hidalgo. Academic Area of Chemistry. Carretera Pachuca-Tulancingo Km. 4.5 Mineral de la Reforma, Hgo., México и <sup>2</sup>Universidad Lasalle Pachuca, Calle Belisario Domínguez 202, Centro, 42000 Pachuca de Soto, Hgo. México

У овом раду изведено је рачунарско хемијско проучавање Наратриптана на X/DGDZVP (где је X = B3LYP, M06, M06L и B97XD) нивоу теорије. Резултати сугеришу постојање два могућа конформера у воденој фази. Израчунавање глобалних и локалних дескриптора реактивности указује да оба конформера имају једнако хемијско понашање. Студије доковања

откривају да се оба конформера везују за TYR359 остатак 5HT<sub>1B</sub> рецептора. Дакле, први конформер се везује за рецептор преко THR209 и THR213 док се други везује преко THR209 и SER 212.

(Примљено 29. децембра 2019, ревидирано 10 априла, прихваћено 11. маја 2020)

#### REFERENCES

1. P. J. Goadsby, R. B. Lipton, M. Ferrari, *N. Engl. J. Med.* **346** (2002) 257 (<https://doi.org/10.1056/NEJMra010917>)
2. M. D. Ferrari, R. R. Klever, G. M. Terwindt, C. Ayata, A. M. J. M. van den Maagdenberg, *Lancet Neurol.* **14** (2015) 65 ([https://doi.org/10.1016/S1474-4422\(14\)70220-0](https://doi.org/10.1016/S1474-4422(14)70220-0))
3. T. Lempert, J. Olesen, J. Furman, J. Waterston, B. Seemungal, J. Carey, A. Bis dorff, M. Versino, S. Evers, D. Newman-Toker, *J. Vestib. Res.* **22** (2012) 167 (<https://doi.org/10.3233/VES-2012-0453>)
4. P. J. Goadsby, A. R. Charbit, A. P. Andreou, S. Akerman, P. R. Holland, *Neuroscience* **161** (2009) 327 (<https://doi.org/10.1016/j.neuroscience.2009.03.019>)
5. G. A. Lambert, *CNS Drug Rev.* **11** (2005) 289 (<https://doi.org/10.1111/j.1527-3458.2005.tb00048.x>)
6. M. M. Johnston, A. M. Rapoport, *Drugs* **70** (2010) 1505 (<https://doi.org/10.2165/11537990-00000000-00000>)
7. S. Akerman, P. R. Holland, P. J. Goadsby, *Nat. Rev. Neurosci.* **12** (2011) 570 (<https://doi.org/10.1038/nrn3057>)
8. F. D. Sheftell, A. M. Rapoport, S. J. Tepper, M. E. Bigal, *Headache* **45** (2005) 1400 (<https://doi.org/10.1038/nrn3057>)
9. S. D. Silberstein, in *Neurology and Clinical Neuroscience*, A. H. V. Schapira, E. Byrne, R. S. J. Frackowiak, Y. Mizuno, S. D. Silberstein, Eds., Mosby Elsevier, Philadelphia, PA, 2007, pp. 739–755 (<https://doi.org/10.1016/B978-0-323-03354-1.50060-2>)
10. Y. Zhou, J. Wang, Y. Xiao, T. Wang, X. Huang, *Curr. Pharm. Des.* **24** (2018) 2375 (<https://doi.org/10.2174/1381612824666180515155425>)
11. A. Islam, K. Shadev, M. V. Redy, M. M. Layek, C. Bhar, *Patent WO* 2006 010078 A2. (<https://patentimages.storage.googleapis.com/ef/4e/7f/4da5fce99e57cb/WO2006010078A2.pdf>)
12. J. L. Gázquez, *J. Mex. Chem. Soc.* **52** (2008) 3 (<http://www.scielo.org.mx/pdf/jmcs/v52n1/v52n1a2.pdf>)
13. P. Geerlings, F. De Proft, W. Langenaeker, *Chem. Rev.* **103** (2003) 1793 (<https://doi.org/10.1021/cr990029p>)
14. R. G. Parr, R. G. Pearson, *J. Am. Chem. Soc.* **105** (1983) 7512 (<https://doi.org/10.1021/ja00364a005>)
15. R. G. Pearson, *J. Chem. Educ.* **64** (1987) 561 (<http://dx.doi.org/10.1021/ed064p561>)
16. R. G. Parr, P. K. Chattaraj, *J. Am. Chem. Soc.* **113** (1991) 1854 (<http://dx.doi.org/10.1021/ja00005a072>)
17. R. G. Pearson, *J. Am. Chem. Soc.* **107** (1985) 6801 (<https://doi.org/10.1021/ja00310a009>)
18. R. G. Parr, R. A. Donnelly, M. Levy, W. E. Palke, *J. Chem. Phys.* **68** (1978) 3801 (<http://dx.doi.org/10.1063/1.436185>)
19. R. G. Parr, L. V. Szentháry, S. Liu, *J. Am. Chem. Soc.* **121** (1999) 1922 (<http://dx.doi.org/10.1021/ja983494x>)
20. P. K. Chattaraj, *Chemical reactivity theory: a density functional view*, First, CRC Press/Taylor & Francis, Boca Raton, Fl, 2009 (ISBN 9781420065435).

21. R. G. Parr, W. Yang, *Density-functional theory of atoms and molecules*, First, Oxford University Press, New York, 1989 (ISBN-10 0195092767).
22. R. G. Parr, W. Yang, *J. Am. Chem. Soc.* **106** (1984) 4049 (<https://dx.doi.org/10.1021/ja00326a036>)
23. W. Yang, W. J. Mortier, *J. Am. Chem. Soc.* **108** (1986) 5708 (<https://dx.doi.org/10.1021/ja00279a008>)
24. J. Z. Vilseck, J. Tirado-Rives, W. L. Jorgensen, *J. Chem. Theory Comput.* **10** (2014) 2802 (<https://doi.org/10.1021/ct500016d>)
25. N. Godbout, D. R. Salahub, J. Andzelm, E. Wimmer, *Can. J. Chem.* **70** (1992) 560 (<https://doi.org/10.1139/v92-079>)
26. A. D. Becke, *J. Chem. Phys.* **98** (1993) 5648 (<http://dx.doi.org/10.1063/1.464913>)
27. A. D. Becke, *Phys. Rev., A* **38** (1988) 3098 (<https://dx.doi.org/10.1103/PhysRevA.38.3098>)
28. Y. Zhao, D. G. Truhlar, *Theor. Chem. Acc.* **120** (2008) 215 (<http://dx.doi.org/10.1007/s00214-007-0310-x>)
29. Y. Wang, X. Jin, H. S. Yu, D. G. Truhlar, X. He, X. H. Designed, X. H. Performed, *PNAS* **114** (2017) 8487 (<http://dx.doi.org/10.1073/pnas.1705670114>)
30. J. Da Chai, M. Head-Gordon, *Phys. Chem. Chem. Phys.* **10** (2008) 6615 (<https://doi.org/10.1039/b810189b>)
31. S. Mierteš, E. Scrocco, J. Tomasi, *Chem. Phys.* **55** (1981) 117 ([https://dx.doi.org/10.1016/0301-0104\(81\)85090-2](https://dx.doi.org/10.1016/0301-0104(81)85090-2))
32. S. Mierteš, J. Tomasi, *Chem. Phys.* **65** (1982) 239 ([http://dx.doi.org/10.1016/0301-0104\(82\)85072-6](http://dx.doi.org/10.1016/0301-0104(82)85072-6))
33. *Gaussian 09*, Revision A.01, Gaussian, Inc., Wallingford, CT, 2009
34. *Gaussview*, Rev. 3.09, Windows version, Gaussian Inc., Pittsburgh, PA
35. M. Thompson (n.d.), <http://www.arguslab.com/arguslab.com/ArgusLab.html> (Accessed September 25, 2019)
36. A.-R. Allouche, *J. Comput. Chem.* **32** (2011) 174 (<https://doi.org/10.1002/jcc.21600>)
37. T. Lu, F. Chen, *J. Comput. Chem.* **33** (2012) 580 (<https://doi.org/10.1002/jcc.22885>)
38. S. Dallakyan, A. J. Olson, *Methods Mol. Biol.* **1263** (2015) 243 ([https://doi.org/10.1007/978-1-4939-2269-7\\_19](https://doi.org/10.1007/978-1-4939-2269-7_19))
39. O. Trott, A. J. Olson, *J. Comput. Chem.* **31** (2010) 455 (<https://doi.org/10.1002/jcc.21334>)
40. E. F. Pettersen, T. D. Goddard, C. C. Huang, G. S. Couch, D. M. Greenblatt, E. C. Meng, T. E. Ferrin, *J. Comput. Chem.* (2004) (<https://doi.org/10.1002/jcc.20084>)
41. L. Schrödinger, *Thomas Hold.* (2015) (<https://doi.org/10.1007/s13398-014-0173-7.2>)
42. R. A. Laskowski, M. B. Swindells, *J. Chem. Inf. Model.* (2011) (<https://doi.org/10.1021/ci200227u>)
43. D. V. R. N. Bhikshapathi, V. D. Madhuri, V. V Rajesham, R. Suthakaran, *Am. J. Pharmtech Res. Res.* **4** (2014) 799 (<http://ajptr.com/archive/volume-4/april-2014-issue-2>)
44. E. R. Johnson, S. Keinan, P. Mori-Sánchez, J. Contreras-García, A. J. Cohen, W. Yang, *J. Am. Chem. Soc.* **132** (2010) 6498 (<https://doi.org/10.1021/ja100936w>)
45. J. L. Gázquez, F. Méndez, *J. Phys. Chem.* **98** (1994) 4591 (<https://doi.org/10.1021/j100068a018>)
46. F. L. Hirshfeld, *Theor. Chim. Acta* **44** (1977) 129 (<http://dx.doi.org/10.1007/BF00549096>).
47. L. Senthilkumar, P. Umadevi, K. N. Nithya, P. Kolandaivel, *J. Mol. Model.* **19** (2013) 3411 (<http://doi: 10.1007/s00894-013-1866-0>).